

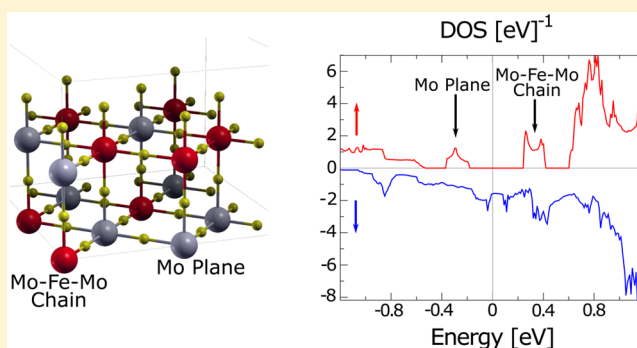
Effect of Cationic Disorder on the Magnetic Moment of $\text{Sr}_2\text{FeMoO}_6$: Ab Initio Calculations

A. M. Reyes,^{*,†,§} Y. Arredondo,[‡] and O. Navarro[†]

[†]Unidad Morelia, Instituto de Investigaciones en Materiales, and [‡]Escuela Nacional de Estudios Superiores Unidad Morelia, Universidad Nacional Autónoma de México, Antigua carretera a Pátzcuaro No. 8701, Col. Ex Hacienda de San José de la Huerta, 58190 Morelia, Michoacán México

[§]Facultad de Ciencias Físico Matemáticas, Universidad Michoacana de San Nicolás de Hidalgo, Av. Francisco J. Múgica S/N, Ciudad Universitaria, Morelia, Michoacán México

ABSTRACT: Discrepancies between both theoretical calculations and experimental measurements of the magnetic moment on Fe sites in $\text{Sr}_2\text{FeMoO}_6$ have been accounted for because of disorder effects. In this work, we deepen the repercussions of cationic disorder in the above ferromagnetic compound specially about the interactions between Fe antisites, which are found antiferromagnetic for the most stable systems. An amount of disorder (12.5% and 25%) was introduced within the systems via atomic substitution. Ab initio calculations using the generalized gradient approximation were performed with local Hubbard terms U_{Fe} and U_{Mo} associated with both Fe and Mo sites, respectively. We found a magnetic saturation of $2.99 \mu_{\text{B}}$ for a 12.5% amount of disorder and $2.22 \mu_{\text{B}}$ in the case of 25% disorder, which is in agreement with neutron magnetic scattering experiments. Half-metallicity is found to remain only for the 12.5% disorder case.



INTRODUCTION

Magnetic materials research has taken brand-new directions with the increasing ability to synthesize materials whose charge carriers show an important spin-polarization. Also, advances in the field of electronics upon miniaturization of devices have served to expose spin-polarization effects. Should the development of fully spin-polarized materials succeed, the field of spintronics would boost the electronic industry with much smaller and robust devices with intrinsic memory. Improvements in decision making via spin-valves,¹ spin-transistors,² nonvolatile storage devices,³ and even quantum computing⁴ are part of the motivation to pursue full comprehension of spin-polarized materials. In this sense, half-metallic ferromagnetic oxides have attracted extensive attention not only as a source of fully spin-polarized charge carrier for spintronic applications but also as potential candidates for magnetoelectronic elements by virtue of their colossal magnetoresistance.^{5,6} In 1998, Kobayashi et al.⁵ reported a large low-field magnetoresistance effect in the double perovskite $\text{Sr}_2\text{FeMoO}_6$ (SFMO) with a fairly high magnetic transition temperature T_{C} of about 415 K which provided intriguing opportunities to explore magnetoelectronic materials showing half-metallic characteristics at room temperature.

SFMO is a material that belongs to the class of double perovskites ($\text{A}_2\text{BB}'\text{O}_6$), where the alkaline-earth ion A is Sr and transition-metal ions B and B' are Fe and Mo, respectively, arranged in a rock-salt structure.⁷ Some comprehension of the

electronic and magnetic properties of such a system in terms of its composition and defects has been achieved. We are especially interested in the experimental value of the saturation magnetization (M_{S}) which is found to be smaller than the theoretical value of $4 \mu_{\text{B}}$ per formula unit (f.u.). Such a result has been related to the presence of cationic disorder in the form of B-site or antisite disorder, that is, when some Fe and Mo atoms interchange their crystallographic positions as a result of the sample preparation parameters.^{6,8} It is known that M_{S} decreases linearly with the increase of antisite disorder;⁸ however, the microscopic origin of the M_{S} decrease is not entirely clear. Both classical Monte Carlo simulations⁹ and ab initio quantum-mechanical band structure analysis^{7,10} indeed predicted a reduction of M_{S} as a function of mis-site disorder, but the underlying reason for this reduction is different in these two approaches. In the first one, it is assumed that M_{S} decreases because of only the antiferromagnetic (AFM) couplings between Fe–O–Fe and Fe–O–Mo and a higher moment of Fe as compared to Mo. Such calculations are supported by experimental results from neutron magnetic scattering which suggest that the smaller value of M_{S} is due to strong AFM interactions between nearest-neighbor Fe cations.¹¹ In this paper, we propose a correlated picture to revisit the effect of

Received: January 5, 2016

Revised: January 15, 2016

Published: January 27, 2016

cationic disorder on the electronic and magnetic properties of the double perovskite SFMO. A structural optimization of the system was performed, and computation of the density of states (DOS) of the systems was carried out from first-principles calculations, within the generalized gradient approximation (GGA) with an effective on-site correlation in Fe and Mo.

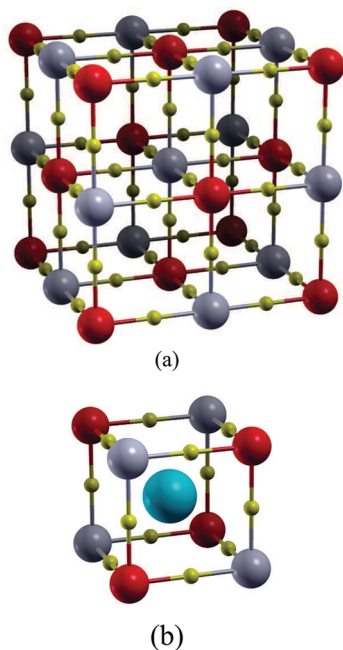


Figure 1. (a) Forty-atom supercell of $\text{Sr}_2\text{FeMoO}_6$. Fe atoms (red) and Mo (gray) atomic sites alternated with O (yellow). (b) A Sr atom is in each cubic subcell.

COMPUTATIONAL DETAILS

The SFMO is a body-centered tetragonal structure, with a space group $I4/mmm$ and lattice parameters $a = b = 5.57 \text{ \AA}$ and $c = 7.90 \text{ \AA}$.⁵ The FeO_6 and MoO_6 in octahedral configuration are alternately organized along the cubic axes, whereas the Sr atoms are located body-centered into the structure.⁵ In Figure 1a, we show a supercell formed by four structures per unitary formula. A single subcell with a centered Sr is shown in Figure 1b.

Calculations were performed with the QUANTUM ESPRESSO package¹² employing density functional theory and Perdew–Burke–Ernzerhoff exchange–correlation functional.¹³ The ultrasoft pseudopotentials RRKJ¹⁴ in the ion–electron interaction were used for the Fe (3d), Mo (4d), and O (2p) ions, and the VAN pseudopotentials¹⁵ were used for the Sr (5s), with semicore electrons included in the valence, as well as a plane-wave basis set for electronic wave functions and charge density, with energy cutoffs of 50 and 200 Ry, respectively. Structural optimizations were calculated with quasi-Newton BFGS preconditioning.¹² The electronic Brillouin zone integration in the self-consistent calculation was found to converge with a $6 \times 6 \times 6$ uniform k-point mesh. For density of states calculation, we sampled a $12 \times 12 \times 12$ uniform k-point mesh and used a Gaussian smearing of 0.02 Ry. We used GGA+U approximation, which allowed us to obtain a correct magnetic ground state for SFMO. An effective on-site correlation was set on Fe and Mo of $U_{\text{Fe}} = 3 \text{ eV}$ and $U_{\text{Mo}} = 1 \text{ eV}$, respectively.¹⁶ Disordered configurations of the SFMO system were simulated upon introduction of antisites, that is, Fe and Mo sites were interchanged. We also tested the case of parallel and antiparallel spin polarization on the Fe antisites.

Calculations were performed by constructing supercells of eight and four formula units. The system with eight formula

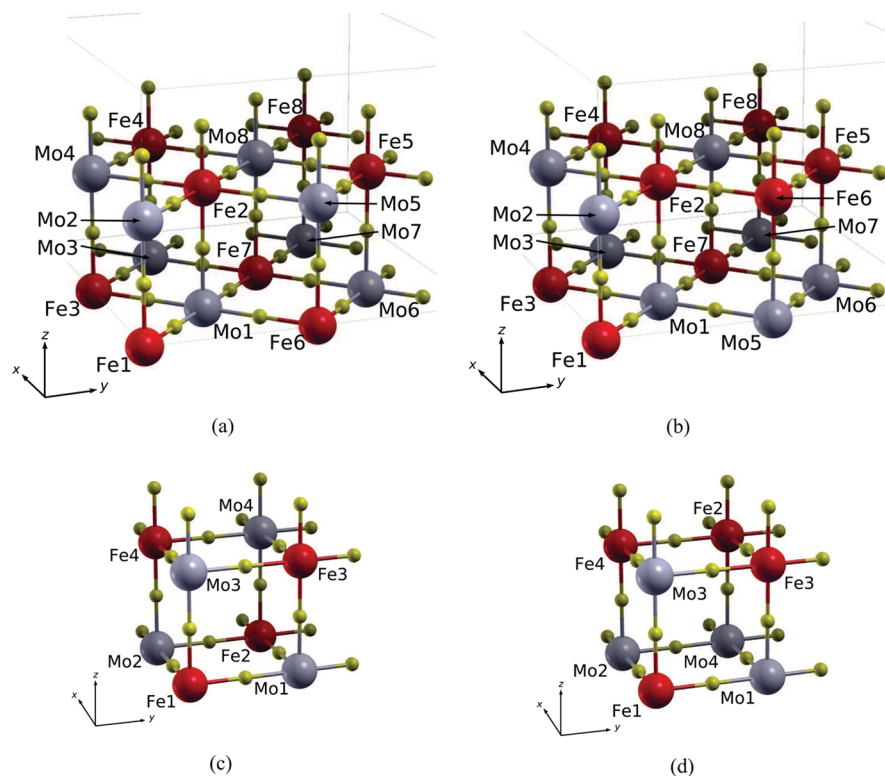


Figure 2. Eighty atom (a) ordered and (b) disordered primitive unit supercells. Forty atom (c) ordered and (d) disordered primitive unit supercells. Fe atoms (red) and Mo (gray) atomic sites alternated with O (yellow). A Sr atom is in each cubic subcell.

units corresponds to an 80 atom supercell (Figure 2a), which allows us to introduce a 12.5% disorder (Figure 2b) with Fe ions in the following sites: Fe1(0, 0, 0), Fe2(0.25, 0.25, 0.5), Fe3(0.5, 0, 0), Fe4(0.75, 0.25, 0.5), Fe5(0.25, 0.75, 0.5), Fe6(0, 0.5, 0), Fe7(0.5, 0.5, 0), and Fe8(0.75, 0.75, 0.5) and Mo ions in Mo1(0.25, 0.25, 0), Mo2(0, 0, 0.5), Mo3(0.75, 0.25, 0), Mo4(0.5, 0, 0.5), Mo5(0, 0.5, 0.5), Mo6(0.25, 0.75, 0), Mo7(0.75, 0.75, 0), and Mo8(0.5, 0.5, 0.5). The later case with four formula units in a 40 atom supercell (Figure 2c) allows us to introduce a 25% disorder (Figure 2d), which approximately corresponds to the experimental systems studied by Sánchez et al.,¹¹ who obtained structures at 15 K with $\sim 70\%$ order and $\sim 18\%$ disorder. The Fe ions were placed in the following sites: Fe1(0, 0, 0), Fe2(0.5, 0.5, 0), Fe3(0, 0.5, 0.5), and Fe4(0.5, 0, 0.5), and Mo ions were placed in Mo1(0, 0.5, 0), Mo2(0.5, 0, 0), Mo3(0, 0, 0.5), and Mo4(0.5, 0.5, 0.5). The effect of positional disorder at Fe/Mo sites is simulated by interchanging Fe and Mo sites, so as to generate different physical environments surrounding each inequivalent Fe and Mo site; indeed, the 12.5% disorder was generated interchanging Fe6 and Mo5 sites (see Figure 2b), and for 25% disorder, we interchanged Fe2 and Mo4 sites (see Figure 2d). Several disorder configurations were tested. Each system was structurally optimized, and total energies were calculated. Our criterion to keep the systems described earlier was based on a lowest-energy and therefore most stable system argument.

RESULTS AND DISCUSSION

As described in the Introduction, the antisite disorder is related to misplaced cations. Antisite disorder and the order of the system are found to be related by $x = (100 - 2y)$, where x and y are the order and disorder percentage, respectively.¹⁷ Our results for 12.5% disorder show that the minimal self-consistent field energy with the Fe antisite with AFM spin orientation is -7376.744 eV and for the Fe antisite with FM spin orientation -7376.704 eV, showing a difference of 0.04 eV. For the later case, with 25% disorder, we found for the Fe antisite with AFM spin orientation an energy value of -7376.413 eV and for the Fe antisite with FM spin orientation an energy value of -7376.379 eV, with a difference of 0.034 eV; the AFM cases are the most probable disordered configurations. Such tetragonal crystalline structures have calculated lattice parameters $a = b = 5.58$ Å, $c = 7.90$ Å and $a = b = 5.57$ Å, $c = 7.69$ Å, respectively. The total magnetic moment of the 12.5% disordered supercell is $2.99 \mu_B$, which is close to the experimental value of $\sim 3.2 \mu_B$,⁶ while that of the 25% disorder is $2.22 \mu_B$, in agreement with the experimental result of $2.2 \mu_B$.¹¹

Within the energy range shown in Figure 3, the total electronic DOS is essentially determined by Fe (3d) and Mo (4d) orbitals. Figure 3a shows the total DOS for the fully ordered SFMO structure where the half-metallic behavior is observed with an up-spin channel gap of 1.06 eV. The total DOS for the 12.5% disordered SFMO system with AFM coupling is shown in Figure 3b, where half-metallicity is maintained, although some electronic states do appear above and below the Fermi level, mostly because of Mo (4d) orbitals in the up-spin channel. Because of an important contribution by Mo5 antisite, the gap is reduced up to 0.44 eV. For the 25% disordered system, the half-metallic feature is broken down in majority ($\sim 75\%$) by Mo (4d) orbitals in the up-spin channel, just as the previous case by the Mo4 antisite, leaving the SFMO compound as a normal paramagnet, with states in both up- and down-spin channels.

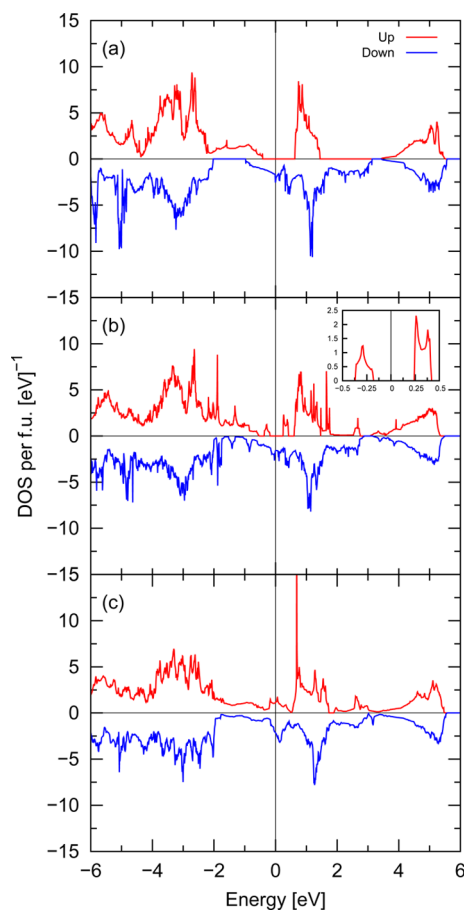


Figure 3. Total density of states (DOS) for (a) fully ordered, (b) 12.5%, and (c) 25% disordered $\text{Sr}_2\text{FeMoO}_6$. Inset b, DOS associated (left) with a Mo plane and (right) to a Mo–Fe–Mo chain.

In Table 1, one observes that the magnetic moments at the Mo antisites are strongly influenced by the number of nearest-neighbor Fe atoms, which is modified directly by disorder. With 12.5% disorder, the magnetic moment value of Mo5 antisite increases from $-0.28 \mu_B$ in the ordered configuration to $-0.03 \mu_B$ and up to $0.17 \mu_B$ in the Mo4 antisite with 25% disorder. On the Fe antisites, the magnetic moment is negative because of the AFM couplings, and its value remains rather stable. We found that, with 12.5% disorder, the Mo5 antisite is ferromagnetically coupled to the Fe6 antisite, while with 25% disorder, the Mo4 antisite is antiferromagnetically coupled to the Fe2 antisite. This interesting behavior could explain the differences between the DOS in the range from -1 to 1 eV.

In an ordered SFMO system, the Mo charge carriers with up-spin state are scattered because of AFM couplings between Fe and Mo sublattices, which allow only down-spin charge transfer via Pauli's exclusion principle. Our calculations for 12.5% disorder show that the Mo5 antisite is coupled ferromagnetically to the Fe6 antisite with a magnetic moment of $-0.03 \mu_B$, allowing superexchange of up-spin itinerant electrons from the Mo plane (i.e., Mo1–Mo5–Mo6 in the primitive unit cell, Figure 2b) through the Mo–Fe–Mo chain (i.e., Mo5–Fe6–Mo5 in the primitive unit cell, Figure 2b), increasing the probability to have Mo up-spin states. However, the Fe sites (i.e., Fe2 and Fe5 in the primitive unit cell, Figure 2b) are antiparallel to Mo up-spin charge carriers, which allows scattering and keeps the half-metallic character of the system. In contrast, with 25%

Table 1. Distribution of Mo and Fe Neighbors at Various Shells for Inequivalent Fe and Mo Sites for the Ordered and Disordered Structures^a

supercell configuration	sites	nearest-neighbors	magnetic moment [μ_B /f.u.]	total magnetic moment [μ_B /f.u.]	total energy per f.u. [eV]
fully ordered	Fe	6 Mo	3.60	4.00	-7376.480
	Mo	6 Fe	-0.28		
12.5% disorder Fe antiseite-AFM	Fe1	6 Mo	3.67	2.99	-7376.744
	Fe2	5 Mo + 1 Fe	3.68		
	Fe3	6 Mo	3.65		
	Fe4	5 Mo + 1 Fe	3.68		
	Fe5	5 Mo + 1 Fe	3.68		
	Fe6	2 Mo + 4 Fe	-3.69		
	Fe7	6 Mo	3.67		
	Fe8	5 Mo + 1 Fe	3.68		
	Mo1	5 Fe + 1 Mo	-0.27		
	Mo2	6 Fe	-0.24		
	Mo3	5 Fe + 1 Mo	-0.27		
	Mo4	6 Fe	-0.31		
	Mo5	2 Fe + 4 Mo	-0.03		
	Mo6	5 Fe + 1 Mo	-0.27		
	Mo7	5 Fe + 1 Mo	-0.27		
	Mo8	6 Fe	-0.24		
12.5% disorder Fe antiseite-FM				4.03	-7376.704
25% disorder Fe antiseite-AFM	Fe1	6Mo	3.64	2.22	-7376.413
	Fe2	4 Fe + 2 Mo	-3.59		
	Fe3	2 Fe + 4 Mo	3.60		
	Fe4	2 Fe + 4 Mo	3.60		
	Mo1	4 Fe + 2 Mo	-0.06		
	Mo2	4 Fe + 2 Mo	-0.06		
	Mo3	6 Fe	-0.25		
Mo4	2 Fe + 4 Mo	0.17			
25% disorder Fe antiseite-FM				3.77	-7376.379

^aThe last three columns show the magnetic moment at various inequivalent sites and total magnetic moment and total energies of self-consistent field calculation.

disorder, the breakdown of the half-metallicity may be explained through AFM coupling between Fe2 and Mo4 antisites and through a major density of antiparallel Fe sites per formula unit, which increases the hopping probability from the Mo plane (i.e., Mo1–Mo4–Mo2 in the primitive unit cell, Figure 2d) to the Mo–Fe–Mo chain (i.e., Mo4–Fe2–Mo4 in the primitive unit cell, Figure 2d) via Pauli's exclusion principle, increasing the up-spin states in the Fermi level. We also argue that the behavior of the DOS of the up-spin channel with 12.5% disorder, in the range from -0.35 eV to -0.18 eV, can be associated with that of a Mo plane and, in the range from 0.25 to 0.41 eV, with that of a Mo–Fe–Mo chain (inset Figure 3b). On the other hand, the DOS of the up-spin channel with 25% disorder (Figure 3c) displays a superposition of both plane and chain, in the range from -0.15 to 0.06 eV, corresponding to that of a Mo–Fe–Mo chain, and the peak at 0.34 eV can be associated with a Mo plane (Figure 3c).

According to neutron diffraction data from disordered SFMO samples,¹¹ disorder would generate Fe–O–Fe and Mo–O–Mo structures such as those shown in Figure 2d. AFM Fe–Fe couplings would then originate from strong superexchange Fe–O–Fe interactions giving rise to the observed magnetic scattering and would account for the smaller magnetic moment of the system reported in Sánchez et al.¹¹ In our model, AFM couplings in the disordered systems were also

preferred over FM ones as found from ground-state energy results. Also, in agreement with Monte Carlo calculations,⁹ our findings further support the scenario where disorder in such systems leads to AFM couplings between neighboring Fe sites, instead of to the FM coupling proposed in refs 7 and 10.

CONCLUSIONS

Our optimized analysis of the ground state of disordered SFMO systems explains the AFM couplings between neighboring Fe sites, in agreement with Monte Carlo calculations⁹ and neutron magnetic scattering experiments.¹¹ The electronic structure shows that at 12.5% of disorder the SFMO system maintains its half-metal character, with the gap reduced from 1.06 to 0.44 eV. Spin-up states appear below the Fermi level because of Mo plane and above the Fermi level because of a Mo–Fe–Mo chain formation; also, the Fe antisite is coupled antiferromagnetically to Fe sites, and its theoretical saturation magnetization changes from 4.0 μ_B to 2.99 μ_B . With 25% disorder, half-metallicity disappears in the SFMO because of the charge transfer from Mo to the Mo–Fe–Mo chain. Also, with Fe antisites coupled antiferromagnetically to Fe sites, the up-spin states at the Fermi level and the theoretical saturation magnetization decreases from 4.0 μ_B to 2.22 μ_B , in agreement with 2.2 μ_B from experimental results.¹¹

■ AUTHOR INFORMATION

Corresponding Author

*E-mail: reyesabdul@iim.unam.mx. Phone: +52 (1) 443 1665 526.

Notes

The authors declare no competing financial interest.

■ ACKNOWLEDGMENTS

This work was partially supported by projects PAPIIT-IN100313 (O.N.) and PAPIIT-IA104915 (Y.A.) from Universidad Nacional Autónoma de México. A.M.R. is grateful to CONACyT for the fellowship. SFMO structures were generated with Kokalj's XCRYSDEN package (<http://www.xcrysden.org/>).

■ REFERENCES

- (1) Singh, S.; Rawat, R.; Muthu, S. E.; D'Souza, S. W.; Suard, E.; Senyshyn, A.; Banik, S.; Rajput, P.; Bhardwaj, S.; Awasthi, A. M.; et al. Spin-Valve-Like Magnetoresistance in Mn_2NiGa at Room Temperature. *Phys. Rev. Lett.* **2012**, *109*, 246601.
- (2) Ohdaira, Y.; Oogane, M.; Naganuma, H.; Ando, Y. Spin Transistor Using Magnetic Tunnel Junctions with Half-Metallic Co_2MnSi Heusler Alloy Electrodes. *Appl. Phys. Lett.* **2011**, *99*, 132513.
- (3) Gould, C.; Schmidt, G.; Molenkap, L. W. In *Spintronics*; Tomasz, D., Awschalom, D. D., Kaminska, M., Ohno, H., Eds.; Elsevier: Amsterdam, 2008; Vol. 82.
- (4) Ohno, H. In *Semiconductors Spintronics and Quantum Computation*; Awschalom, D. D., Loss, D., Samarth, N., Eds.; Springer-Verlag: Berlin, 2002.
- (5) Kobayashi, K.-I.; Kimura, T.; Sawada, H.; Terakura, K.; Tokura, Y. Room-Temperature Magnetoresistance in an Oxide Material with an Ordered Double-Perovskite Structure. *Nature* **1998**, *395*, 677–680.
- (6) Topwal, D.; Sarma, D. D.; Kato, H.; Tokura, Y.; Avignon, M. Structural and Magnetic Properties of $\text{Sr}_2\text{Fe}_{1+x}\text{Mo}_{1-x}\text{O}_6$ ($-1 \leq x \leq 0.25$). *Phys. Rev. B: Condens. Matter Mater. Phys.* **2006**, *73*, 094419.
- (7) Saha-Dasgupta, T.; Sarma, D. D. *Ab initio* Study of Disorder Effects on the Electronic and Magnetic Structure of $\text{Sr}_2\text{FeMoO}_6$. *Phys. Rev. B: Condens. Matter Mater. Phys.* **2001**, *64*, 064408.
- (8) Balcells, L.; Navarro, J.; Bibes, M.; Roig, A.; Martínez, B.; Fontcuberta, J. Cationic Ordering Control of Magnetization in $\text{Sr}_2\text{FeMoO}_6$ Double Perovskite. *Appl. Phys. Lett.* **2001**, *78*, 781.
- (9) Ogale, A. S.; Ogale, S. B.; Ramesh, R.; Venkatesan, T. Octahedral Cation Site Disorder Effects on Magnetization in Double-Perovskite $\text{Sr}_2\text{FeMoO}_6$: Monte Carlo Simulation Study. *Appl. Phys. Lett.* **1999**, *75*, 537–539.
- (10) Stoeffler, D.; Colis, S. Oxygen Vacancies or/and Antisite Imperfections in $\text{Sr}_2\text{FeMoO}_6$ Double Perovskites: an *Ab Initio* Investigation. *J. Phys.: Condens. Matter* **2005**, *17*, 6415.
- (11) Sánchez, D.; Alonso, J. A.; García-Hernández, M.; Martínez-Lope, M. J.; Martínez, J. L.; Mellergård, A. Origin of Neutron Magnetic Scattering in Antisite-Disordered $\text{Sr}_2\text{FeMoO}_6$ Double Perovskites. *Phys. Rev. B: Condens. Matter Mater. Phys.* **2002**, *65*, 104426.
- (12) Giannozzi, P.; Baroni, S.; Bonini, N.; Calandra, M.; Car, R.; Cavazzoni, C.; Ceresoli, D.; Chiarotti, G. L.; Cococcioni, M.; Dabo, I.; et al. QUANTUM ESPRESSO: a Modular and Open-Source Software Project for Quantum Simulations of Materials. *J. Phys.: Condens. Matter* **2009**, *21*, 395502.
- (13) Perdew, J. P.; Burke, K.; Ernzerhof, M. Generalized Gradient Approximation Made Simple. *Phys. Rev. Lett.* **1996**, *77*, 3865–3868.
- (14) Rappe, A. M.; Rabe, K. M.; Kaxiras, E.; Joannopoulos, J. D. Optimized Pseudopotentials. *Phys. Rev. B: Condens. Matter Mater. Phys.* **1990**, *41*, 1227–1230.
- (15) Vanderbilt, D. Soft Self-Consistent Pseudopotentials in a Generalized Eigenvalue Formalism. *Phys. Rev. B: Condens. Matter Mater. Phys.* **1990**, *41*, 7892–7895.
- (16) Suárez, J.; Estrada, F.; Navarro, O.; Avignon, M. Magnetic Properties of the Ordered and Disordered Double Perovskite $\text{Sr}_2\text{Fe}_{1+x}\text{Mo}_{1-x}\text{O}_6$ ($-1 \leq x \leq 1/3$). *Eur. Phys. J. B* **2011**, *84*, 53–58.
- (17) Mandal, T. K.; Greenblatt, M. In *Functional Oxides*; Bruce, W. B., O'Hare, D., Walton, R. I., Eds.; John Wiley & Sons: West Sussex, U.K., 2010.